Atmos. Chem. Phys. Discuss., 9, 17429–17463, 2009
www.atmos-chem-phys-discuss.net/9/17429/2009/

Atmospheric Chemistry and Physics Discussions

This discussion paper is/has been under review for the journal *Atmospheric Chemistry and Physics (ACP)*. Please refer to the corresponding final paper in *ACP* if available.

Regional N_2O fluxes in Amazonia derived from aircraft vertical profiles

M. T. S. D'Amelio[1], L. V. Gatti[1], J. B. Miller[2,3], and P. Tans[2]

[1]Instituto de Pesquisas Energéticas e Nucleares (IPEN), São Paulo, Brazil
[2]National Oceanic and Atmospheric Administration (NOAA), Colorado
[3]Cooperative Institute for Research in Environmental Sciences (CIRES), University of Colorado, Colorado

Received: 14 July 2009 – Accepted: 3 August 2009 – Published: 20 August 2009

Correspondence to: M. T. S. D'Amelio (monicatais@yahoo.com)

Published by Copernicus Publications on behalf of the European Geosciences Union.

Abstract

Nitrous oxide (N_2O) is the third most important anthropogenic greenhouse gas. Globally, the main sources of N_2O are nitrification and denitrification in soils. About two thirds of the soil emissions occur in the tropics and approximately 20% originate in wet rainforest ecosystems, like the Amazon forest. The work presented here involves aircraft vertical profiles of N_2O from the surface to 4 km over two sites in the Eastern and Central Amazon: Tapajós National Forest (SAN) and Cuieiras Biologic Reserve (MAN), and the estimation of N_2O fluxes for regions upwind of these sites. To our knowledge, these regional scale N_2O measurements in Amazonia are unique and represent a new approach to looking regional scale emissions. The fluxes upwind of MAN exhibited little seasonality, and the annual mean was 2.1 ± 1.0 mg N_2O m^{-2} day^{-1}, higher than that for fluxes upwind of SAN, which averaged 1.5 ± 1.6 mg N_2O $m^{-2}day^{-1}$. The higher rainfall around the MAN site could explain the higher N_2O emissions. For fluxes from the coast to SAN seasonality is present for all years, with high fluxes in the months of March through May, and in November through December. The first peak of N_2O flux is strongly associated with the wet season. The second peak of high N_2O flux recorded at SAN occurs during the dry season and can not be easily explained. However, about half of the dry season profiles exhibit significant correlations with CO, indicating a larger than expected source of N_2O from biomass burning. The average CO:N_2O ratio for all profiles sampled during the dry season is 94 ± 77 mol CO:mol N_2O and suggests a larger biomass burning contribution to the global N_2O budget than previously reported.

1 Introduction

Nitrous oxide (N_2O) is the third most important anthropogenic greenhouse gas with a global warming potential about 310 times higher than CO_2 over a 100-year time-horizon. Currently, its radiative forcing is about 10% that of CO_2 (Hofmann, 2006). Its atmospheric lifetime is estimated to be 120 years (Schindlbacher et al., 2004; IPCC,

ACPD

9, 17429–17463, 2009

2007). It also contributes to stratospheric ozone depletion (Cicerone, 1989). The most important N_2O sink (90%) is photodissocation above 30 km, with reaction with excited oxygen (10%) accounting for the balance. The atmospheric N_2O mixing ratio has been increasing from 270 ppb in 1750 to about 321 ppb in 2007, an increase of 19% (Fluckiger et al., 2002). The average annual growth rate from 1999 to 2000 was 0.85±1.1 ppb yr^{-1} (IPCC, 2007) and 0.73±0.06 ppb yr^{-1} from 1988–2005 (Hirsch, et al., 2006). The main reason is the increase in anthropogenic sources, like land use (N-fertilization) and industry, and current estimates are that about 40% of total N_2O emissions are anthropogenic (IPCC, 2007). The IPCC Fourth Assessment report (AR4) estimates 60% of total N_2O anthropogenic contribution (6.7 Tg N yr^{-1}) is from agricultural soils (1.7 to 4.8 Tg N yr^{-1}). Others authors have published that direct N_2O emissions from agricultural soils contribute about 77% of total anthropogenic contribution, with 6.2 Tg N yr^{-1} (Prather and Ehhalt, 2001; Del Grosso et al., 2005; Hirsch et al., 2006) of 8.0 Tg N yr^{-1} (Kroeze et al., 1999; Hirsch et al., 2006).

Globally, the main sources of N_2O are nitrification and denitrification in soils (6.6 Tg N yr^{-1}) and the ocean (3.8 Tg N yr^{-1}) (IPCC, 2007; Flückiger, et al., 2002). About two thirds of the soil emissions occur in the tropics and approximately 20% are though to originate in wet rainforest ecosystems (Van Haren et al., 2005; Keller et al., 1993; Melillo et al., 2001). Other sources include gas-phase oxidation of NH_3, and industrial sources such as adipic acid and nitric acid production (0.7 Tg N yr^{-1}) and biomass burning (0.7 Tg N yr^{-1}) (Thiemens and Troggler 1991; IPCC, 2007). In tropical land, the main sources are likely to be natural soils with 3.3 Tg N yr^{-1} to 9.0 Tg N yr^{-1} (IPCC, 2007) (16.4 Tg N yr^{-1} for Chapuis-Lardy, et al., 2007), followed by agricultural soils with 1.7 Tg N yr^{-1} to 4.8 Tg N yr^{-1} (IPCC, 2007) (4.2 Tg N yr^{-1} for Chapuis-Lardy, et al., 2007), which are in agreement with others authors that rain forests emit a large amount of N_2O (Keller et al., 1993, Melillo et al., 2001). Many studies in tropical forests, like the Amazon forest (Borchert, 1998; Jipp et al., 1998), agree that the average N_2O flux in these forests is much greater in the wet than dry season (Van Haren et al., 2005; Verchot et al., 1999; Perez et al., 2000; Garcia-Montiel

ACPD
9, 17429–17463, 2009

et al., 2003; Wick, et al., 2005; Kiese et al., 2003). The soil source strength for N_2O is determined by the availability of substrates and the activity of nitrifying/denitrifying microbial communities, and on soil diffusivity, which is controlled mainly by soil water (Neftel et al., 2000; Smith et al., 2003), and on concurrent N_2O consumption process (Cavigelli and Robertson, 2001). Soil moisture conditions (Wick et al., 2005), temperature and pH (Huang et al., 2004; Wick et al., 2005) are some parameters that affect the rate of N_2O emission, naturally or in agricultural systems (Maggioto et al., 2000).

Studies in three different agricultural treatments in central Rondônia, Brazil, reported emissions ranging from −11.3 to 324.3 mg N_2O m^{-2} day^{-1} (Passianoto et al. 2003). Globally, Mosier et al. (1998) estimated emissions of 8.5 Tg N yr^{-1} for agricultural soils.

Many authors have also reported N_2O uptake by soil, although some have attributed the uptake to measurement uncertainty and have dismissed those results (Chapuis-Lardy et al., 2007; Donoso er al., 1990). However, other research studies considered N_2O consumption by denitrifiers under high soil water contents and low soil temperature (Ryden, 1981; Glatzel and Stahr, 2001), low soil NO_3^- and N concentration (Rosenkranz et al., 2005), low pH (Knowles, 1982), and other factors. Others studies observed different conditions for N_2O soil uptake, such as high temperature (Yamulki et al., 1995) or high pH (Bremner and Blackmer, 1980), for example. This N_2O soil uptake could have important repercussions for quantifying the global source and the atmospheric lifetime of N_2O.

Studies in Amazonian forests have shown that primary forests emit significantly more N_2O than a pasture or unfertilized agriculture area (Do Carmo et al., 2005; Garcia-Montiel et al., 2003; Wick, et al., 2005; Verchot et al., 1999). However, do Carmo et al. (2005) observed that N treatments of pasture soils emitted about 10 times more N_2O than primary forest.

The work presented here involves aircraft vertical profiles of N_2O from 305 m to about 4 km (a.s.l.), over two sites in the Eastern and Central Amazon: Tapajós National Forest, near Santarém in the state of Pará; and Cuieiras Biologic Reserve, near Manaus in the state of Amazonas (Fig. 1). N_2O measurements over this 4 km altitude range

are sensitive to fluxes over a large upwind fetch because of the strong and persistent trade winds, which is most likely to be the region between the sites and the Atlantic coast. To our knowledge, these regional scale N_2O measurements in Amazônia are unique and represent a new approach to looking regional scale emissions. In addition to the inherent uncertainties of extrapolation of inventory or "bottom-up" flux estimates, the major difference between our "top-down" approach and extrapolation is that our regional measurements implicitly integrate over all possible sources and sinks. This means that our measurements can constrain the total flux of N_2O, but without necessarily revealing much information on what processes may have contributed to the total. We apply a column integration technique (Miller et al., 2007) to estimate total surface emissions of N_2O and compare these fluxes to previous top-down and bottom up estimates for Amazonia and the tropics.

2 Methods

Above Tapajós National Forest (site code SAN), around 70 km south of Santarém, Pará, (since December 2000) and Cuieiras Biological Reserve (site code MAN), around 50 km north of Manaus, Amazonas (since December 2004), air samples have been collected with semi-automatic portable sampling systems consisting of a portable flask package (PFP) which is shipped between the field site and laboratory and a portable compressor package (PCP), which remains at the site. The PFP contains 17 glass flasks with automated stopcocks and a logic controller board, and the PCP contains two pumps and batteries to power both the PCP and PFP. Each unit is contained within an aluminum suitcase. These two units are loaded into a light aircraft and a sampling inlet is stuck out of either the pilot window (MAN) or a wing vent (SAN) to connect the compressor unit to external air. To collect samples, the pilot uses a wired remote control allowing him to sample at pre-determined altitudes. The flights between 2000 and 2005 consisted of one descending and one ascending spiral vertical profile from 3660 m to 305 m and 305 m to 3600 m, over two locations separated by 30–100 km.

ACPD
9, 17429–17463, 2009

Profiles obtained since 2006 are only descending from 4270 m to 305 m over just a single location for both sites, allowing for better vertical sampling resolution. From 2000 to 2003, flasks units with samples collected in Brazil were sent to the NOAA/ESRL laboratory in Boulder, CO USA, where they were analyzed for CO_2, CH_4, N_2O, SF_6, CO and H_2. Since 2004, a replica of NOAA analysis system for those gases has been operating at Instituto de Pesquisas Energéticas e Nucleares (IPEN) in São Paulo, SP Brazil. This analytical system is the Multiple Analysis of Gases Climate Change (MAGICC).

The N_2O and SF_6 analysis system is an ECD (Electron Capture Detector) chromatograph (HP 6890 Plus + model) with pre-column of 6 ft, 3/16" o.d. 100/120 mesh Haysep Q and a column of 6 ft, 3/16" o.d. 100/120 mesh Haysep Q and a 15 ml volume sample loop. This system also uses a 10 port valve to inject the sample loop to pre-column, then just after the N_2O and SF_6 gas arrive to the column, the 10 port valve turns and starts a back flush in the pre-column to remove other gases. The carrier gas used in this system is an Argon/CH_4 (5% of CH_4) mixture.

MAGICC/IPEN has a mean repeatability for N_2O of 0.1 ppb (Fig. 2) as determined from the standard deviation of 20 consecutive aliquots from a high pressure cylinder of ambient air, which is very similar to that obtained at the NOAA lab (0.2 ppb). MAGICC/IPEN stability and precision was calculated analyzing the prepared tank CA05558 (blue in Fig. 2) which was analyzed periodically since 2004 and each time, we analyzed 20 aliquots. The variation of the means of the analyses in a given day is the repeatability. Since 2007 we added the periodic analyses of another tank calibrated at NOAA, CA04533 (red in Fig. 2). We also used this CA04533 tank to make an inter-comparison between the two laboratories (NOAA/ESRL and IPEN – Atmospheric Chemistry Laboratory (LQA)). The mean value of calibration at IPEN was 318.9±0.3 ppb N_2O and the calibration at NOAA was 318.8±0.2 ppb N_2O. This inter-comparison provides important evidence that after 2003, when the replica analysis system started makes the analysis, there is only a small artifact associated with this change. The standard gases used in the analysis are prepared by NOAA, and the inter-comparison program is continuous.

In addition to our sites in Brazil, we used measurements on air samples collected at Ascension Island (ASC 7°55′S, 14°25′W) and Barbados, Caribbean (RPB 13°12′N, 59°24′W) as part of the NOAA Earth System Research Laboratory (NOAA/ESRL) global air sampling network. This air was sampled into 2.5 l glass flasks with Teflon-tipped glass stopcocks and filled to about 1.2 bar (Conway et al., 1994), and shipped to NOAA for analysis to laboratory.

At SAN, the ascending profiles were made above the Tapajós National Forest (02°51′S, 5°58′W), near the "km 67" tower that is located around 7 km to the east of the Tapajós river. Descending profiles were made 30 km to the east of the tower, above an agriculturally impacted area (02°52′S; 54°41′W), in order to assess the impact of possible local influences. At MAN, descending profiles were made above the "K34" eddy covariance tower at Cuieiras Biological Reserve (2°35′S, 60°12′W) 50 km north of Manaus (population 1.8 million), and ascending profiles were made 100 km east (typically upwind) of the tower, above undeveloped forest (2°30′S, 59°05′W). 20 km east from tower, i.e., between the 2 sites, there is the road and farmers. The comparison between preserved area and tower site was made to assess possible influence of farms, transport and the city of Manaus.

At both sites, differences between ascending and descending profiles were generally small compared to differences with the marine background, showing that local influence relative to that between the sites and the coast was negligible (Fig. 3). In order to sample the vertical structure of the background air for Amazon basin, between 2000 and 2003, several vertical profiles were collected 50 km northeast of Fortaleza, state of Ceará (site code FTL 4°09′S, 38°16′W), in the Atlantic coast of Brazil. All sampled sites are indicated at Fig. 1, where open circles are marine boundary layer (MBL) background sites and filled circles are vertical profile sites within Brazil.

3 Results

In order to analyze the N_2O time series (Fig. 4), it is necessary define a background N_2O mixing ratio representing the air entering Brazil off the Atlantic Ocean. This helps to remove the global and tropical trends that influence N_2O within the Amazon basin. Air entering the Amazon basin is dominated by trade-wind easterlies coming from the tropical Atlantic Ocean, with relative influence of Northern and Southern Hemisphere air which depends upon the seasonally varying latitude of the Inter-Tropical Convergence Zone (ITCZ). Considering this seasonality, two NOAA monitoring station were chosen to represent air from each hemisphere: RPB and ASC. Between 2000 and 2003, 10 vertical profiles over FTL were also collected. A comparison of these flights with RPB and ASC time series shows that FTL is bounded by ASC and RPB, confirming that air from both hemispheres influence the Amazon basin background.

The profiles show the integrated impact of N_2O surface emissions for the areas between the Atlantic coast and the sampling sites. Analyzing Fig. 4, we observe that before 2004 the eastern Amazon N_2O mixing ratio was generally between that of the two background sites, indicating only modest additions to the zonal background from Amazonian fluxes. However, since 2004 N_2O mixing ratios over SAN and MAN were higher than background by 0.7 and 1.0 ppb, on average, respectively. Notably, this is significantly higher than 0.1 ppb, which is the difference of calibration between NOAA and IPEN, indicating that the observed difference can not be explained by the analysis laboratory change. The largest enhancements are in the convective boundary layer (CBL; which we define here as altitudes less than 1200 m a.s.l.) (Fig. 4b), although there are noticable enhancements in the free troposphere (Fig. 4a), possibly indicating the convective redistribution of N_2O emitted into the CBL. The higher N_2O mixing ratios in the CBL indicate surface flux of N_2O by these two regions in Amazonia. The differences between our SAN or MAN measurements and the Atlantic background can be used to quantify N_2O fluxes.

Because of strong convection one cannot count on surface emissions to be trapped

in the CBL, so we use a column integration technique (Miller et al., 2007) that does not distinguish the CBL and free troposphere. To apply the column integration technique, we estimate the background N_2O mixing ratio representing the air entering Brazil off the Atlantic Ocean using sulfur hexafluoride (SF_6, a purely anthropogenic gas) as a transport tracer, because the relative Northern and Southern Hemisphere contributions to the N_2O background vary and depend on the seasonally varying latitude of the ITCZ. SF_6 has no regional sources or sinks in Amazon basin (Olivier, 1999), so we consider the SF_6 mixing ratio in the Amazon Basin as the same as that of the air entering Brazil. Figure 5 shows that the vast majority of the time SF_6 at SAN and MAN is bounded by the time series from ASC and RPB. Using a simple two-end-member mixing model, we then calculate the fractions of air arriving at our Amazonian sites that can be represented by the background sites ASC and RPB, and can then be applied to any other conserved tracer (Eqs. 1 and 2) (Miller et al., 2007).

$$\mathrm{ASC}_{(\mathrm{SITE})} = 1 - \mathrm{RPB}_{(\mathrm{SITE})} = \frac{\mathrm{SF}_{6(\mathrm{SITE})} - \mathrm{SF}_{6(\mathrm{RPB})}}{\mathrm{SF}_{6(\mathrm{ASC})} - \mathrm{SF}_{6(\mathrm{RPB})}} \quad (1)$$

$$X_{bg} = \mathrm{ASC}_{\mathrm{SITE}} \cdot X_{\mathrm{ASC}} + \mathrm{RPB}_{\mathrm{SITE}} \cdot X_{\mathrm{RPB}} \quad (2)$$

$\mathrm{ASC}_{(\mathrm{SITE})}$ and $\mathrm{RPB}_{(\mathrm{SITE})}$ represents the ASC and RPB fraction, respectively, for a specific site; $\mathrm{SF}_{6(\mathrm{SITE})}$ represents the SF_6 mixing ratio for each specific site (SAN or MAN), and $\mathrm{SF}_{6\,\mathrm{ASC\,or\,RPB}}$, is the SF_6 mixing ratio at ASC and RPB, respectively. X_{bg} represents the background mole fraction of the gas (N_2O in this case) for a specific site (SAN or MAN); and X_{ASCorRPB} is the mixing ratio at ASC or RPB. Note that we do not bound the values of $\mathrm{ASC}_{\mathrm{site}}$ between 0 and 1, which assumes that the SF_6 and N_2O gradients between ASC and RPB extend further north and south beyond the background sites. Figure 6 presents four example original and "corrected" N_2O vertical profiles in different years for SAN and MAN to illustrate the SF_6-based background subtraction process.

We calculated the N_2O flux from the eastern Amazon basin by integrating the N_2O mixing ratio difference (coast to sample site) shown in Fig. 6b from the surface to the

ACPD
9, 17429–17463, 2009

top of the profile according to Eq. (3) (Miller et al., 2007) for each profile. This flux represents the flux contribution from the coast to the sample site.

$$F_{N_2O} = \frac{\int_{z_i}^{z_f} [(X_{N_2O})_{SITE} - (X_{N_2O})_{bg}] dz}{t} \quad (3)$$

Here, X_{N_2O} is the concentration in units of mol m^{-3}, which can be determined from observations and estimated vertical profiles of temperature and pressure. z_i and z_f are the minimum and maximum range of vertical integration that is defined between altitudes of profile, ground level to top of profile. t was determined for each altitude, counting the time (in days) the air took to travel between the coast and the sampling site in the back trajectory simulated by the Hysplit model (Fig. 7) (Draxler, 2003 – www.arl.noaa.gov/ready/open/hysplit4.html). Note that when a back trajectory reached low altitudes (<50 m a.g.l.) before the coast, or in other instances where trajectories could not be calculated, a default value of 2 was used for t. This is an improvement over the approach of Miller et al. (2007), who used a constant value for t of 2±1 days. However, sensitivity tests for both CH_4 and N_2O showed that using a nominal value of 2 days did not significantly affect the annual or seasonal flux averages. The back trajectory simulated by Hysplit model confirms for both sites the initial statement and the SF_6 observations that air from both Hemispheres enters the basin. Air arriving at the sites above 3000 m appears to originate from a narrower north-south band centered on the equator.

Uncertainty in SF_6 and N_2O values at ASC and RPB used in Eqs. 1 and 2 are 0.05 ppt and 0.34 ppb, respectively, based on the scatter about smooth curve fits in Fig. 4 (shown by the gray error band). Uncertainty in $(X_{N_2O})_{site}$ in Eq. 3 is the measurement uncertainty of 0.2 ppb and $(X_{N_2O})_{bg}$ is 0.26 ppb, as determined by propagating uncertainties through Eqs. (1) and (2). The F_{N_2O} uncertainty is estimated by propagating uncertainty from all term in Eqs. (1)–(3) and is typically 0.72 mg N_2O m^{-2} day^{-1}.

Our analysis requires combining measurements from two labs; therefore calibration

as well as comparison of actual samples become very important. We made two kinds of comparisons between the IPEN and NOAA laboratories, and sensitivity tests were made in order to examine possible bias between NOAA and IPEN. In addition to the tank comparison mentioned above, which showed a difference of 0.1±0.3 ppb, another comparison was made by analyzing flasks sampled at the Arembepe site (site code ABP 12°58′S, 38°30′W) in 2008. In the same day, two flasks were sampled for NOAA and two sampled for IPEN with a difference of 20–40 min between them. This comparison shows a bias between IPEN and NOAA of 0.3±0.5 ppb, in average. This comparison is significantly noisier than the tank inter-comparison as seen by the 0.5 ppb uncertainty in the difference. The period used in this comparison corresponds to 2008, due to likely sampling problems in 2006 and 2007 at Arembepe. As a sensitivity test, we consider the larger difference of 0.3 ppb from the Arembepe inter-comparison. To test the impact of a possible sampling bias on our analysis, after 2004 we subtracted 0.3 ppb from the IPEN measurements and recalculated the fluxes. As expected, the mean fluxes were smaller, but the ratios between seasons and sites were not strongly affected, as shown in Table 1.

The fluxes calculated from all profiles from the coast to SAN or MAN are plotted in Fig. 8a and b, respectively. The flux climatology exhibits significant seasonality for SAN. There are two times of the year that show high fluxes: March until May, and November and December. For fluxes from coast to MAN, the seasonality is less pronounced with the maximum emissions centered on April. However, the annual mean flux between the coast and MAN is 2.1±1.0 mg N_2O m^{-2} day^{-1}, which is higher than that for the coast to SAN, which is 1.6±1.4 mg N_2O m^{-2} day^{-1}. Variability of the fluxes, expressed as the standard deviation of individual means is significant. It is larger than the uncertainty for a single flux calculation (~0.72) for an individual flux estimate. Although the mean value for MAN is higher, the flux variability for SAN is higher, which reflects the greater seasonality of fluxes upwind of SAN. The higher seasonal flux variability seen at SAN most likely reflects the stronger seasonality in precipitation seen in eastern Amazonia (Fig. 8c).

Soil emission is the most important contribution to N_2O flux (6.6 Tg N yr^{-1}) (IPCC, 2007) and occurs by activity of nitrifying/denitrifying microbial communities in soil (Chapuis-Lardy, et al., 2007; Davidson et al., 2004; Garcia-Montiel et al., 2003; Passianoto et al. 2003). In some regions of Amazon basin, an additional contribution could be agricultural processes (2.8 Tg N yr^{-1} globally) (IPCC, 2007), mainly in Pará, where significant forrest conversion has occurred over the past 10 years. The direct ocean influence was removed when the background was subtracted, and is expected to be significantly smaller than soil or agrictultural emissions. Both the soil emission and agricultural sources can be influenced by soil water and thus precipitation. To see if precipitation could explain the seasonal flux patterns inferred from the MAN and SAN observations, we calculated monthly mean precipitation for a) SAN b) MAN and c) the average of seven sites (Belém, Breves, Cametá, Itacoatiara, Porto de Moz, Souré, Tucuruí) upwind of SAN and MAN (Fig. 8c). All rainfall data were obtained from Instituto Nacional de Meteorologia (INMET: www.inmet.gov.br) and were composed of data from 2001–2007.

Comparing fluxes and rainfall (Fig. 8) it is evident that the first peak of N_2O flux at SAN appears strongly related to wet season precipitation. The flux peak derived from MAN data also corresponds to high rainfall. Furthermore, the higher rainfall in Amazonas, even during the dry season (August to December), could contribute to the high value of N_2O emission that persists throughout the year. Plot-scale studies have also observed a relationship between precipitation and N_2O flux (e.g., Cattannio et al., 2002, Do Carmo et al., 2005).

We studied the fluxes classifying them by the season (Fig. 9). For SAN we classified fluxes into wet (W), transition wet to dry (W/D) and dry (D) seasons. For MAN we separated fluxes only into wet and dry seasons. All the classifications were made based on local precipitation (Fig. 8c). For SAN the months classification are: 1. W: January to May, 2. W/D: June and July, 3. D: August to December. In some years there was a delay in the beginning of wet season in January so that some profiles of this month were classified as dry season. For MAN the month classifications are:

W: November to May, D: June to October. With this classification, we observe less variability in fluxes derived from MAN data than from SAN data. For fluxes based on SAN data, a strong seasonality is evident. In Fig. 8, we note the presence of negative fluxes, which we do not interpret as uptake signals, but most likely occur due to incorrect specification of the background. Our simple model is sensitive to such errors and the fluxes calculated using Eq. 3 are best interpreted in the climatological sense, as displayed in Fig. 9. For MAN data, no negative fluxes are calculated which probably reflects the high mean fluxes recorded there. Like the mean values, the uncertainty in our method means that we can not interpret the variability shown in Fig. 8a and b as actual flux variability. From the coast to SAN, during the dry and wet seasons N_2O fluxes were similar and lower during the transition season. From the coast to MAN, during the wet season N_2O fluxes are higher than dry season, with a more gradual transition to the dry season than is seen at SAN. Comparing fluxes derived from observations at each site, during the wet season, fluxes derived from MAN are almost 0.5 mg N_2O m^{-2} day^{-1} higher than those at SAN. This behavior is very different during dry season, when both places exhibit similar fluxes. From the coast to SAN, we expected the same dry season behavior observed from coast to MAN, i.e., decrease of fluxes relative to the wet season. The high N_2O flux during the dry season over the trajectories from the coast to SAN suggests the presence of a source other than soil emissions. Back trajectories in Fig. 7 show that air arriving at MAN tends to be from the east and northeast, whereas air arriving at SAN tends to be from the east and southeast. Areas east and southeast of SAN are more agriculturally developed than areas northeast of MAN which are more heavily forested. This difference in landscape could be related to the different seasonal patterns and absolute amounts of N_2O flux derived from the measurements at each site.

In addition to seasonal variability, we also observe substantial interannual variability in the fluxes recorded at SAN. For example, our observations indicate lower than average fluxes in 2002, which is consistent with the plot-scale observations of Davidson et al. (2004) that showed a decrease of more than 50% in 2002 compared to the wet

ACPD
9, 17429–17463, 2009

seasons of 2000 and 2001. In contrast, fluxes from 2005 were much higher than average. There is only a weak relationship (r^2 = 0.22) between year to year variations in precipitation (as measured at Santarem) and upwind N_2O emissions. Regardless of the cause of the variations, the large degree of variability in both seasonal and interannual fluxes emphasizes the necessity of long-term monitoring of atmospheric N_2O in Amazonia.

Another important N_2O source could be biomass burning, which at the global scale is estimated to account for only 4% of all emissions (IPCC, 2007). We compared N_2O and CO vertical profiles in order to see if biomass burning might be a significant contributor to dry season N_2O fluxes recorded at SAN. CO has been used as an atmospheric tracer of biomass burning at a variety of scales (Langenfelds, 2002; Gerbig, 2003; van der Werf, 2004). A commonly used compilation of emission ratios (Andreae and Merlet, 2001) gives a best guess biomass burning emission ratio for tropical forests of 817 mol CO/mol N_2O. This suggests very little N_2O is emitted from fires (as in the global budgets). However, in some of our vertical profiles we found evidence for a significant relationship between N_2O and CO in the dry season (Fig. 10). From the total of 25 profiles sampled during the SAN dry season, 28% (7 profiles) exhibited correlations higher than 0.5 and a mean ratio of 99.0±89.8 mol CO/mol N_2O, nearly an order of magnitude larger than Andreae and Merlet (2001). 44% (11 profiles) exhibited correlations higher than 0.3 with a mean ratio of 100.6±68.9 mol CO:mol N_2O. The average ratio of all 25 profiles during the dry season, is 93.8±76.6 mol CO:mol N_2O. However, poor or negative correlations between CO and N_2O were also observed in the dry season, indicating that dry season emissions other than biomass burning may also be required to explain our dry season flux maximum observed at SAN. As a rough estimate of the global N_2O emissions from biomass burning, consistent with our observed ratios, we scale N_2O biomass burning emissions to those of CO. Taking a global biomass burning estimate of 3.53 Pg C yr^{-1} (van der Werf et al., 2004) and an average CO:C molar emission ratio of 0.075 (Andreae and Merlet, 2001), we estimate global CO emissions from biomass burning of 618 Tg CO yr^{-1}. Given our average observed of about 100 mol mol^{-1} for

ACPD
9, 17429–17463, 2009

CO:N_2O, we estimate N_2O biomass burning emissions of 3.1 Tg N yr^{-1} assuming that tropical emission ratios for N_2O and CO are similar to the global flux-weighted average, which is reasonable considering that most biomass burning is tropical. Our results suggest that biomass burning emissions of N_2O may be a significantly larger contributor to the tropical and global N_2O budgets than previously thought.

We interpret our flux results to be representative of large regions, namely the ~10^5–10^6 km^2 area between the sites and the Atlantic coast. If our fluxes were in fact more locally representative, then we would expect the lowest altitudes measured to contain the majority of the signal. In order to test this, we conducted sensitivity tests to assess the influence of the lower altitudes on our flux calculations. We integrated the fluxes from four different starting altitudes to 4270 m: 152 m, 300 m, 600 m and 1000 m. The last altitude was chosen to represent the mid or upper CBL, and the first one (172 m) the control altitude representing the default integration. The variation between flux values from the four starting altitudes was less than 5%, which suggests a regional influence for our fluxes. In general, we also expect that our flux estimates are biased low, because the upper limit of our integral does not fully capture all convective redistribution of flux, which in the Amazon basin may extend all the way toward the tropopause near 15 km. However, based on the shapes of our observed profiles, which often show distinct differences between the CBL and free troposphere, we do not expect that our flux estimates are significant underestimates.

One important way to interpret our fluxes is by comparing our regional flux values to plot-scale fluxes from Amazonian forest and pasture sites, and global-scale estimates (Table 2): both bottom-up (Bouwman, et al., 1995) and top-down (e.g. Hirsch et al., 2006; Huang et al, 2008) sources. In general, N_2O fluxes reported at a variety of scales show general agreement, despite significant variability in the fluxes. Comparing to plot-scale fluxes, differences can be expected as a result of the site-specific conditions for each plot-scale study. For example, looking just at the fluxes from the south-western Amazonian state of Rondonia (RO in Table 2), fluxes vary from 0.1 to 4.3 mg N_2O m^{-2} day^{-1}. The large site to site variability seen at the plot scale might also help to explain

ACPD
9, 17429–17463, 2009

the high variability of our fluxes, because our fluxes will be influenced to some extent by all ecosystems between the coast and the sample site. This is especially true in the case of SAN, where the upwind landscape is composed of undisturbed forest, pasture, fertilized agricultural land and to the southeast, some grassland. Thus, changes in wind or the behavior in any one of these ecosystems could significantly influence our observations. In addition to the annual fluxes, our regional flux results are also similar to the seasonality observed in plot-scale fluxes. The study of Davidson et al. (2004), in particular, shows a very strong N_2O flux response to moisture. This is the case both for the comparison of the throughfall exclusion and control areas and within the normal wet-dry transition within the control area. Neil et al. (2005) studied different forests in Rondônia. Although two of six primary forests studied showed the same (Cacaulandia) or higher (Porto Velho) N_2O fluxes in the dry season compared to wet, the overall pattern was still that of higher N_2O fluxes during the wet season. The fact that some plot-scale studies do show elevated dry season fluxes could help explain our observation of high dry season N_2O fluxes that are not correlated with high CO. In addition to the correlation between N_2O and CO during the dry season, we plotted CO fluxes (calculated in the same way as the N_2O fluxes) vs. N_2O fluxes for SAN and MAN (Fig. 11) for all profiles sampled during this season. We observed three kinds of correlation for upwind of SAN. First, there are a set of sampling days where a clear relationship between CO and N_2O fluxes exist. There are also days in which we see high N_2O with only moderate CO fluxes and also high CO fluxes, with small N_2O fluxes. The causes of N_2O dry season flux variability observed at SAN can not be explained by biomass burning alone, and our analysis suggests that a variety of processes are likely responsible for the variability. In contrast, for data from MAN we did not observe any correlation for CO and N_2O during dry season.

Our regional estimates are also consistent with large scale bottom-up and top-down estimates (Table 2). Our estimates based on MAN and SAN data are higher than the GEIA bottom-up estimates, but more similar to the top-down estimates of Hirsch et al. (2006), who used marine boundary layer atmospheric N_2O data to optimize the

GEIA fluxes using an inverse model. The correspondence of our regional flux estimates with the larger scale N_2O flux estimates confirms the importance of Amazonia in the global N_2O budget.

4 Conclusions

Considering the mean of the all studied years, the region between the coast and MAN presented higher N_2O fluxes (2.1 ± 1.0 mg N_2O m^{-2} day^{-1}) than the region between the coast and SAN (1.5 ± 1.6 mg N_2O m^{-2} day^{-1}), which is consistent with the higher rainfall upwind of MAN, including during the dry season (August to December). The seasonal and interannual variability present in our data suggests that long term measurements covering all seasons are required to understand the dynamics of N_2O emissions in Amazonia.

We calculated large seasonality in the fluxes from SAN for all years, with high fluxes in the months of March through May, and in November through December. Based on the recorded precipitation seasonality and previous plot scale studies the wet season N_2O emissions are likely dominated by forest soil emission accelerated by soil moisture. The unexpectedly high N_2O emission during the dry season, however, suggests a combination of biomass burning and other sources. The low emission ratios between CO and N_2O we observed averaging 94 ± 77 ppb CO/ppb N_2O also suggest that at global scales the importance of biomass burning to the N_2O budget may be underestimated.

Acknowledgements. The authors thank A. Crotwell for support.

References

Andreae, M. O. and Merlet, P.: Emission of trace gases and aerosols from biomass burning, Global Biogeochem. Cy., 15(4), 955–966, 2001.

Borchert, R.: Responses of tropical trees to rainfall seasonality and its long-term changes, Climatic Change, 39, 381–393, 1998.
Bouwman, A. F., van der Hoek, K. W., and Olivier, J. G. J.: Uncertainties in the global source distribution of nitrous oxide, J. Geophys. Res., 100, 2785–2800, 1995.
Bremmer, J. M. and Blackman, A. M.: Mechanisms of nitrous oxide production in soils, in: Biochemistry of Ancient and Morden Environment, edited by: Trudinger, P. A., Walter, M. R., Ralph, R. J., Australian Academy of Science, Canberra, Australia, 1980.
Cattannio, J. H., Davidson, E. A., and Nepstad, D. C.: Unexpected results of a pilot throughfall exclusion experiment on soil emissions of CO_2, CH_4, N_2O, and NO in eastern Amazonia, Biol. Fert. Soils, 36, 102–108, 2002.
Cavigelli, M. A. and Robertson, G. P.: Role of denitrifier diversity in rates of nitrous oxide consumption in a terrestrial ecosystem, Soil Biol. Biochem., 15, 531–536, 2001.
Chapuis-Lardy, L., Wrage, N., Metay, A., Chottes, J.-L. and Bernouxs, M.: Soils, a sink for N_2O? A review, Glob. Change Biol., 13, 1–17, 2007.
Cicerone, R. J.: Analysis of sources and sinks of atmospheric nitrous-oxide (N_2O), J. Geophys. Res.-Atmospheres, 94(D15), 18265–18271, 1989.
Conway, T. J., Tans, P. P., Waterman, L. S., and Thoning, K. W.: Evidence for interannual variability of the carbon-cycle from the national-oceanic-and-atmospheric-administration climate-monitoring-and-diagnostics-laboratory global-air-sampling-network, J. Geophys. Res.-Atmospheres, 99(D11), 22831–22855, 1994.
Coolman, R. M.: Nitrous Oxide Emissions from Amazonian Ecosystems, Ph.D. dissertation, North Carolina State University, available at: http://www2.lib.ncsu.edu/catalog/record/NCSU859296, 1994.
Davidson, E. A., Ishida, F. Y. and Nepstad, D. C.: Effects of an experimental drought on soil emissions of carbon dioxide, methane, nitrous oxide, and nitric oxide in a moist tropical forest, Glob. Change Biol., 10, 2582–2590, 2004.
Del Grosso, S. J., Mosiera, A. R., Partonb, W. J. and Ojimab, D. S.: DAYCENT model analysis of past and contemporary soil N_2O and net greenhouse gas flux for major crops in the USA, Soil Till. Res., 83, 9–24, 2005.
Do Carmo, J. B., Andrade, C. A., Cerri, C. C. and Piccolo, M. C.: Nitrogen availability and N_2O fluxes from pasture soil after herbicide application, R. Bras. Ci. Solo, 29, 735–746, 2005.
Donoso, L., Santana, R., and Sanhueza, E.: Seasonal variation of N_2O fluxes at a tropical savannah site: soil consumption of N_2O during the dry season, Geophys. Res. Lett., 20(13),

1379–1382, 1993.
Draxler, R. R. and Rolph, G. D.: HYSPLIT (HYbrid Single-Particle Lagrangian Integrated Trajectory) Model access via NOAA ARL READY Website (http://www.arl.noaa.gov/ready/hysplit4.html). NOAA Air Resources Laboratory, Silver Spring, MD, 2003.
Flückiger, J., Monnin, E., Stauffer, B., Schwander, J. and Stocker, T.F.: High-resolution Hlocene N_2O ice core record and its relationship with CH_4 and CO_2, Global Biogeochem. Cy., 16 (1),1010, 2002.
Garcia-Montiel, D., Steudler, P. A., Piccolo, M., Neill, C., Melillo, J., and Cerri, C. C.: Nitrogen oxide emissions following wetting of dry soils in forest pastures in Rondônia, Brazil, Biogeochem. J., 64, 319–336, 2003.
Gerbig, C., Lin, J. C., Wofsy, S. C., Daube, B. C., Andrews, A. E., Stephens, B. B., Bakwin, P. S. and Grainger C. A.: Toward constraining regional-scale fluxes of CO_2 with atmospheric observations over a continent: 2. Analysis of COBRA data using a receptor-oriented framework, J. Geophys. Res., 108, D24, doi:10.1029/2003JD003770, 2004.
Glatzel, S. and Stahr, K.: Methane and nitrous oxide exchange in differently fertilized grassland in southern Germany, Plant Soil, 231, 21–35, 2001.
Hirsch, A.I., Michalak, A. M., Bruhwiler, L. M., Peters, W., Dlugokencky, E. J. and Tans, P. P.: Inverse modeling estimates of the global nitrous oxide flux from 1998-2001, Global Biogeochem. Cy., 20, GB1008, doi:10.1029/2004GB002443, 2006.
Hofmann, D. J., Butler, J. H., Dlugokencky, E. J., Elkins, J. W., Masarie, K., Montzka, S. A. and Tans, P.: The role of carbon dioxide in climate forcing from 1979 to 2004: introduction of the Annual Greenhouse Gas Index, Tellus, 58(5), 614–619, 2006
Huang, J., Golombek, A., Prinn, R., Weiss, R., Fraser, P., Simmonds, P., Dlugokencky, E. J., et al.: Estimation of regional emissions of nitrous oxide from 1997 to 2005 using multinetwork measurements, a chemical transport model, and an inverse method, J. Geophys. Res., 113, D17313, doi: 10.1029/2007 JD009381, 2008.
Huang, Y., Zou, J., Zheng, X., Wang, Y., and Xu, X.: Nitrous oxide emissions as influenced by anebdment of plant residues with different C:N ratios, Soil Biol. Biochem., 36, 973–981, 2004.
Intergovernmental Panel on Climate Change – Climate change 2007: The Physical Science Basis. Contribution of Working Group I to the Fourth Assessment Report of Intergovernmental Panel on Climate Change, edited by: Solomon, S., Qin, D., Manning, M., Marquis, M., Averyt, K., Tignor, M. M. B., Miller Jr., H. L. and Chen, Z. Cambridge University Press,

Cambridge, UK, 95–127, 131–206, 501–546, 2007.
Jipp, P. H., Nepstad, D. C., Cassel, D. K. and De Carvalho, C. R.: Deep soil moisture storage and transpiration in forests and pastures of seasonally-dry Amazonia, Climatic Change, 39, 395–412, 1998
Keller, M., Veldekamp, E., Weitz, A. M., and Reiners, W. A.: Pasture age effects on soil-atmosphere trace gas exchange in a deforested area of Costa Rica, Nature, 365, 244–246, 1993.
Kiese, R., Hewett, B., and Graham, A.: Seasonal variability of N_2O emissions and CH_4 uptake by tropical rainforest soils of Queensland, Australia, Global Geochem. Cy., 17, 1043, doi: 10.1029/2002GB002014, 2003.
Knowles, R.: Denitrification Microbiological Reviews, 46, Denitrification, Microbiol. Mol. Biol. R., 46, 43–70, 1982., 1982.
Kroeze, C., Mosier, A. and Nouwman, L.: Closing the global N_2O budget: A retrospective analysis 1500–1994, Global Biogeochem. Cy., 13(1), 1–9, 1999.
Langenfelds, R. L., Francey, R. J., Pak, B. C., Steele, L. P., Lloyd, J., Trudinger, C. M., and Allison C. E.: Interannual growth rate variations of atmospheric CO_2 and its delta C-13, H-2, CH_4, and CO between 1992 and 1999 linked to biomass burning, Global Biogeochem. Cy., 16(3), 1048, 2002.
Maggiotto, S. R., Webb, J. A., Waggner-Riddle, C., and Thurtell, G. W.: Nitrous and nitrogen oxide emissions from turfgrass receiving different forms of nitrogen fertilizer, J. Environ. Qual., 29, 621–630, 2000.
Melilo, J., Steudler, P. A., Feigl, B. J., Neill, C., Garcia-Montiel, D. C., Piccolo, M. C., Cerri, C. C. and Tian, H.: Nitrous oxide emissions from forest and pastures of various ages in the Brazilian Amazon, J. Geophys. Res., 106, 34179–34188, 2001.
Miller, J. B., Gatti, L. V., D'Amelio, M. T. S. et al.: Airborne measurements indicate large methane emissions from the eastern Amazon basin, J. Geophys. Res., 34(10), L10809, doi:10.1029/2006GL 029213, 2007.
Mosier, A., Kroeze, C., Nevison, C., et al.: Closing the global N_2O budget: nitrous oxide emissions trough the agricultural nitrogen cycle, Nutr. Cycl. Agroecosys., 52, 225–248, 1998.
Neftel, A., Blatter, A., Schimid, M., et al.: An experimental determination of the scale lenght of N_2O in the soil of grass-land, J. Geophys. Res., 105, 12095–12103, 2000.
Neill, C., Steudler, P. A., Garcia-Montiel, D. C., Melillo, J. M., Feigl, B. J., Piccolo, M. C. and Cerri, C. C.: Rates and controls of nitrous oxide and nitric oxide emissions following conver-

sion of forest to pasture in Rondônia, Nutr. Cycl. Agroecosys., 71, 1–15, 2005.
Oliver, J. G. J., Bouwman, A. F., Berdowski, J. J. M., Veldt, C., Bloos, J. P. J., Visschedijk, A. H. J., van de Maas, C. W. M. and Zandweld, P. Y. J.: Sectoral emission inventories of greenhouse gases for 1990 on per country basis as well as on 10×10, Environ. Sci. Policy, 2, 241–264, 1999.
Passianoto, C. C., Ahrens, T., Feigl., B. J., Steudler, P. A., do Carmo, J. B., and Melilo, J. M.: Emissions of CO_2, N_2O, and NO in conventional and no-till management oractices in Rondônia, Brazil, Biol. Fert. Soils, 38, 200–208, doi:10.1007/s00374-003-0653-y, 2003.
Perez, T., Trumbore, S. E., Tyler, S. C. et al.: Isotopic variability of N_2O emissions from tropical forest soils, Global Biogeochem. Cy., 14, 525–535, 2000.
Prather, M. and Ehhalt, D.: Atmospheric chemistry and greenhouse gases: Climate Change 2001: The Scientific Basis, edited by: Houghton, J. T., Ding, Y., Noguer, M., van der Linden, P. J., et al., Cambridge University Press, New York, 239–287, 2001.
Rosenkranz, P., Brüggemann, N., Papen, H., Xu, Z., Seufert, G., and Butterbach-Bahl, K.: NO_2, NO and CH_4 exchange, and microbial N turnover over a Mediterranean pine forest soil, Biogeosciences Discuss., 2, 673–702, 2005, http://www.biogeosciences-discuss.net/2/673/2005/.
Ryden, J. C.: N_2O exchange between a grassland soil and the atmosphere, Nature, 292, 235–237, 1981.
Schindlbacher, A., Zechmeister-Boltenstern, S., and Butterbach-Bahl, K.: Effects of soil moisture and temperature on NO, NO_2 and N_2O emissions from European forest soils, J. Geophys. Res., 109, D17302, doi:10.1029/2004JD004590, 2004.
Smith, K. A., Ball, T., Conen, F., et al.: Exchange of greenhouse gases between soil and atmosphere interactions of soil physical factors and biological processes, Eur. J. Soil Sci., 54, 779–791, 2003.
Stehfest, E. and Müller, C.: Simulation of N_2O emissions from a urine-affected pasture in New Zealand with the ecosystms model DayCent, J. Geophys. Res., 109, D03109, doi:10.1029/2003JD004261, 2004.
Thiemens, M. H. and Trogler, W. C.: Nylon production – an unknown source of atmospheric nitrous-oxide, Science, 251, 932–934, 1991.
Van der Werf, G. R., Randerson, J. T., Collatz, G. J., Giglio, L., Kasibhatla, P. S., Arellano, Jr., A. F. Olsen, S. C., and Kasischke, E. S.: Continental-Scale Partitioning of Fire Emissions During the 1997 to 2001 El Nino/La Nina Period, Science, 303(5654), 73–76, 2004.

Van Haren, J. L. M., Handley, L. L., Biel, K. Y., Kudeyarov, V. N., Mclain, J. E. T., Martens, D. A., and Colodner, D. C.: Drought-induced nitrous oxide flux dynamics in an enclosed tropical forest, Global Change Biol., 11, 1247–1257, 2005.

Verchot, L. V., Davidson, E. A., Cattannio, J. H. et al.: Land use and biogeochemical controls of nitrogen oxide emissions from soils in eastern Amazonia, Global Biogeochem. Cy., 13, 31–46, 1999.

Wick, B., Veldkamp, E., de Mello, W. Z., Keller, M., and Crill, P.: Nitrous oxide fluxes and nitrogen cycling along a pasture chronosequence in Central Amazonia, Brazil, Biogeosciences Discuss., 2, 499–535, 2005, http://www.biogeosciences-discuss.net/2/499/2005/.

Yamulki, S., Goulding, K. W. T., Webster, C. P. and Harisson, R. M.: Studies on NO and N_2O fluxes from a wheat field, Atmos. Environ., 29, 1627–1635, 1995.

Table 1. Sensitivity of the possible bias between NOAA and IPEN labs.

	SAN		MAN	
Flux (mg $N_2O\,m^{-2}\,day^{-1}$)	WET	DRY	WET	DRY
Original	1.45±1.4	1.72±1.4	2.53±0.9	1.56±0.8
Original −0.3 ppb	0.94±1.2	1.13±1.1	1.68±0.8	1.10±1.0
difference	0.51±2.6	0.59±2.5	0.85±1.5	0.46±1.8
	In space (SAN/MAN)		Over time (WET/DRY)	
			SAN	MAN
Original	1.01		1.18	1.65
Original −0.3 ppb	1.23		1.46	1.93
difference	18%		19%	14%

ACPD
9, 17429–17463, 2009

Table 2. Comparison of N_2O fluxes in global, regional and plot scale at Amazon Brazilian Basin.

Ecosystem/Location	Period	Season	Flux(mg N_2O $m^{-2}day^{-1}$)
Global-scale			
GEIA tropical land[1]	1990	Annual	0.95
Hirsch et al. tropical land[1]	1998–2001	Annual	1.54±0.55
GEIA South America[1]	1990	Annual	1.55
Hirsch et al. South America[1]	1998–2001	Annual	2.50±0.89
Hirsch et al. South America [1]	2002–2005	Annual	1.6±0.5
Regional-scale			
Coast to SAN[2]	2001–2007	Wet	1.42±1.62
Coast to SAN[2]	2001–2007	Dry	1.62±1.69
Coast to MAN[2]	2004–2007	Wet	2.73±1.15
Coast to MAN[2]	2004–2007	Dry	1.94±1.56
Plot-scale			
PF Porto Velho, RO[3]	1992–1999	Wet; Dry	(1.5±0.4); (2.3±0.4)
PF Jamari, RO[3]	1992–1999	Wet; Dry	(3.4±1.0); (1.6±0.4)
PF Caucalândia, RO[3]	1992–1999	Wet; Dry	(2.6±0.4); (2.5±0.4)
PF Novo Vida, RO[3]	1992–1999	Wet; Dry	(1.9±0.4); (1.3±0.3)
PF Ouro Preto, RO[3]	1992–1999	Wet; Dry	(4.1±1.8); (1.8±0.2)
PF Manaus, AM[4]	1992–1999	Annual	0.4
PF SAN, PA[5a]	2001–2002	Annual	1.3±0.2
PF SAN, PA[5b]	2001–2002	Annual	2.2±0.9
PF SAN, PA[5c]	2000–2002	Wet; Dry	4±2; 1±0.5
PF Santarém, PA[6]	1999/2000	Annual	2.9–4.1
PF Nova Vida, RO[7]	2001	Annual	4.0±0.8
YP RO[4]	1992–1999	Annual	2.7–4.34
YP Nova Vida, RO[7]	2001	Annual	0.2±0.1
OP RO[4]	1992–1999	Annual	0.1–0.3
TA Nova Vida, RO[7]	2001	Annual	0.6±0.3

[1]Hirsch et al., 2006, average of scenarios A,B,C,D,G; S. American totals derived by scaling tropical land totals by ratio of tropical S. American to tropical land flux in GEIA. ; [2]This study; [3]Neil et al., 2005; [4]Coolman, 1994; [5]Davidson et al., 2004 [a]exclusion treatment, [b]control, wet and dry season from control treatment (uncertainty represents interannual variability); [6]Wick et al., 2005; [7]Do Carmo et al., 2007; [8]Stehfest and Müller, 2004. PF = Primary Forest; YP = Young Pasture; OP = Old Pasture; TA = Treatment Area

Fig. 1. Map of sampling sites used in this study. Open circles are marine boundary layer (MBL) background sites and filled circles are vertical profile sites within Brazil (Miller et al., 2007).

ACPD

9, 17429–17463, 2009

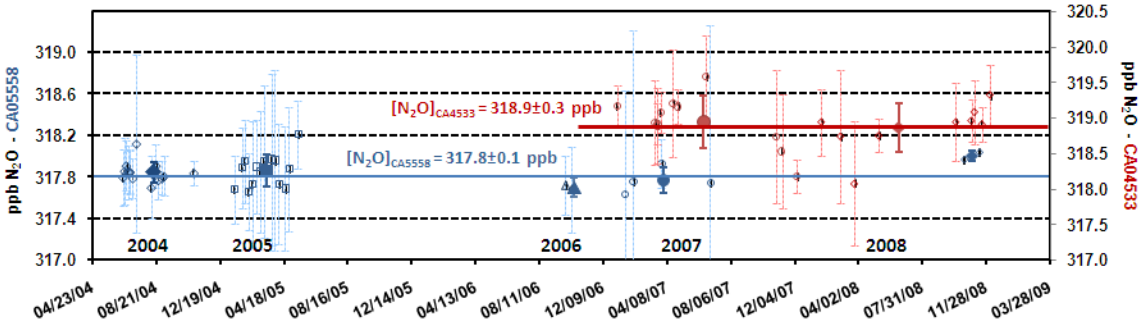

Fig. 2. N_2O times series for the tanks CA05558 (blue points) and CA04533 (red points). Each small point represents the mean of 20 aliquots for the tanks, and the error bars represent the one sigma standard deviation of the 20 analyses (repeatability). The large filled symbols represent the mean of all analyses for a given calendar year. The stability of the blue points, especially, demonstrates the long-term stability and precision of our system (reproducibility).

ACPD
9, 17429–17463, 2009

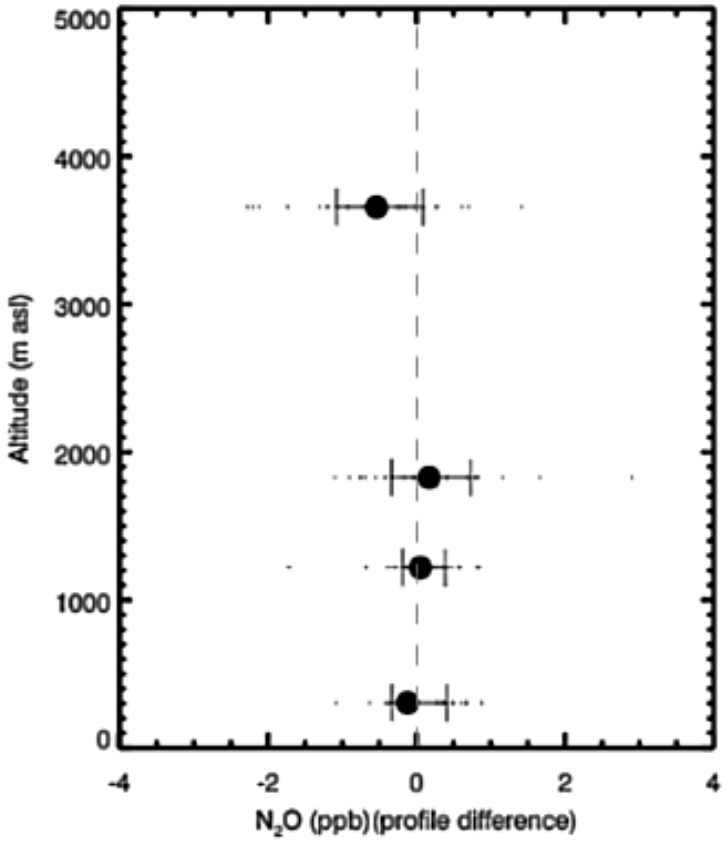

Fig. 3. Differences between ascending and descending profiles at SAN. The error bars show the 25th and 75th percentiles of the differences between the profiles at SAN. The small dots are the individual differences. The median values (50th percentiles) are the large symbols.

ACPD
9, 17429–17463, 2009

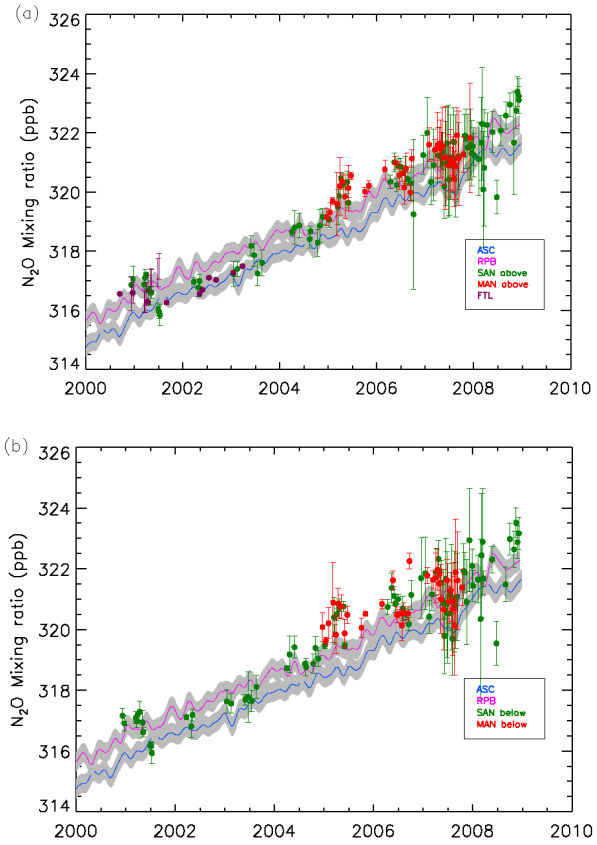

Fig. 4. N_2O Time Series, Marine boundary layer sites ASC, RPB (thin lines) and FTL, SAN and MAN vertical profile average **(a)** above 1000 m and **(b)** bellow 1000 m.

ACPD
9, 17429–17463, 2009

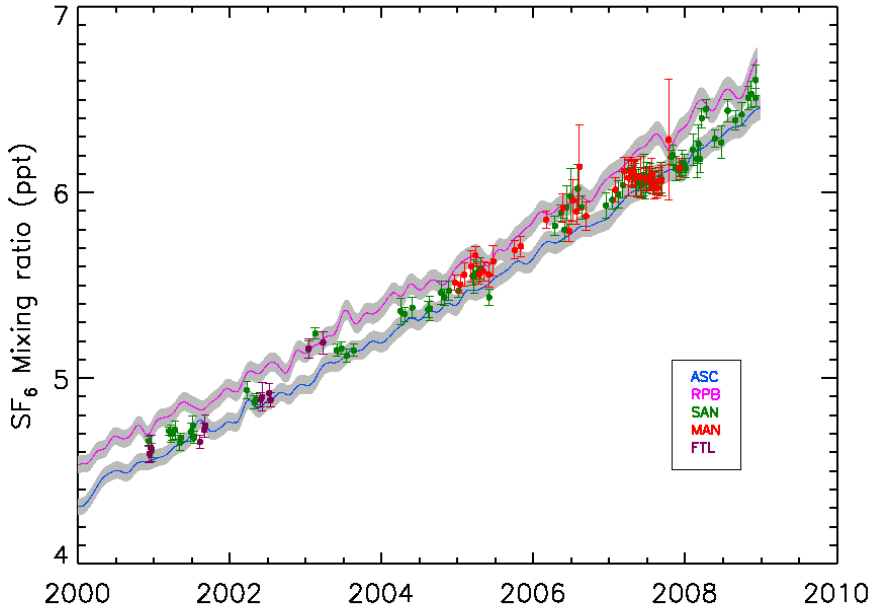

Fig. 5. SF_6 Time Series. Marine boundary layer sites ASC, RPB (thin lines); FTL, MAN and SAN vertical profiles means.

ACPD
9, 17429–17463, 2009

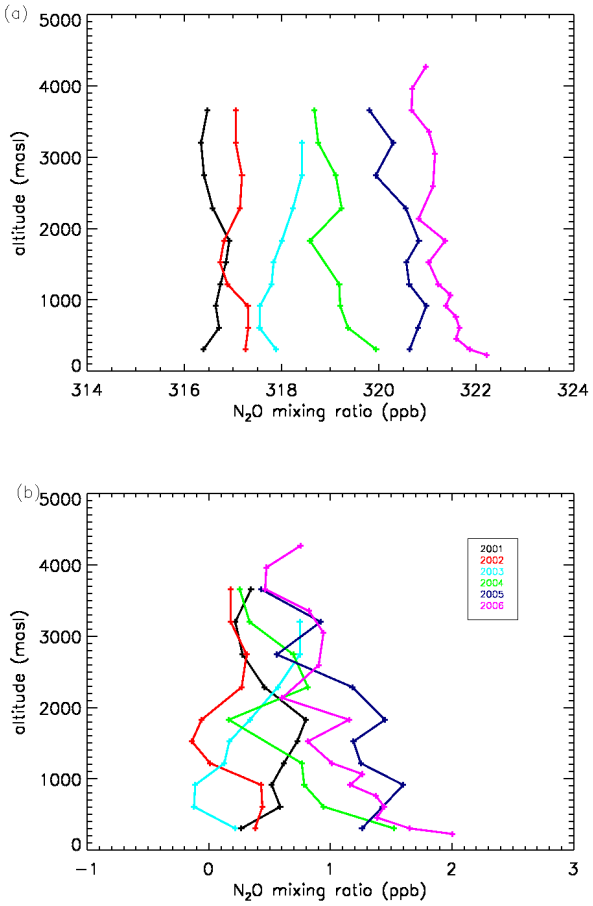

Fig. 6. Six sample N_2O vertical profiles for different years (2001–2006): **(a)** raw data and **(b)** with background subtracted, thus removing the global and/or regional trends.

ACPD

9, 17429–17463, 2009

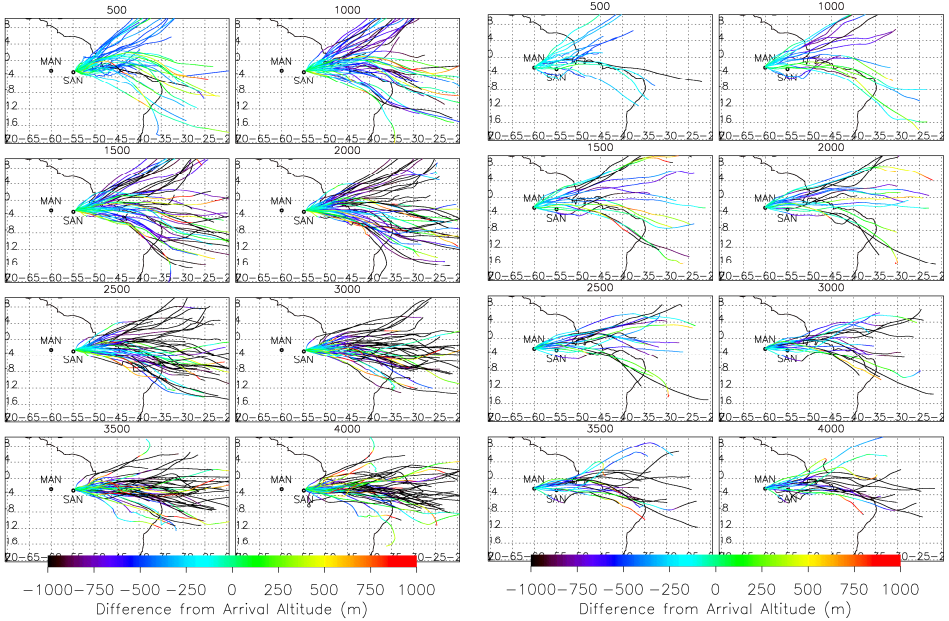

Fig. 7. Back trajectories for **(a)** SAN and **(b)** MAN for altitudes from 500 to 4000 m each 500 m, used to estimate the time *t* which air masses took to travel from the coast to the sampling site, obtained with Hysplit back-trajectory model (Draxler, 2003 – www.arl.noaa.gov/ready/open/hysplit4.html.) used to calculate N_2O flux. The colorbar represents the difference from the arrival altitude (shown as the title of the plot) at any point along the trajectory.

ACPD
9, 17429–17463, 2009

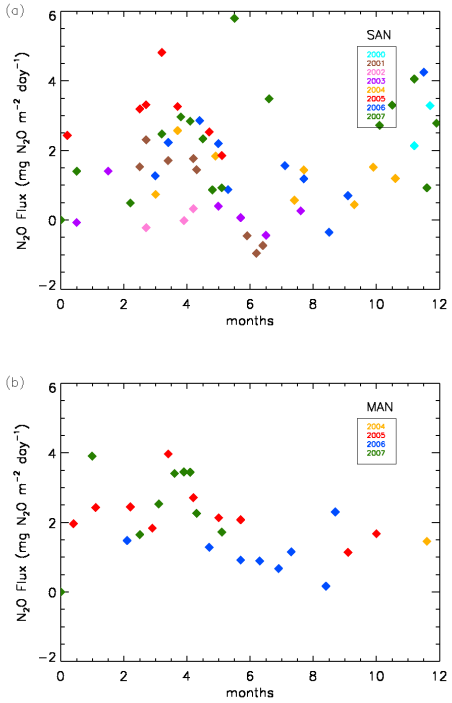

Fig. 8. N_2O Fluxes upwind of **(a)** SAN between 2000 and 2007 and **(b)** MAN between 2004 and 2007. **(c)** Average rainfall for SAN (blue), MAN (red) and seven sites (yellow) located upwind of the sample sites: Belém, Breves, Cametá, Itacoatiara, Porto de Moz, Souré, Tucuruí (INMET – http://www.inmet.gov.br). The averages were calculated using data between 2001 and 2007 for SAN and "Other sites" and 2004 to 2007 for MAN. The error bars represent the standard deviation across years.

ACPD
9, 17429–17463, 2009

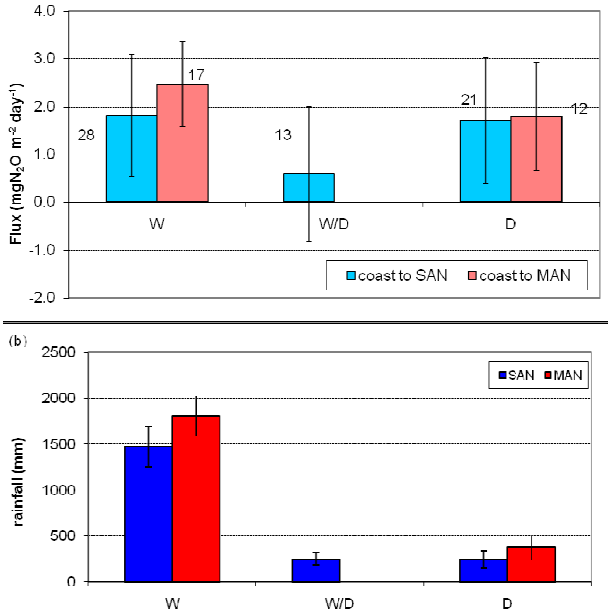

Fig. 9. Trimester (three-month) average **(a)** N_2O fluxes from coast to SAN and MAN for all studied years, **(b)** rainfall for SAN (blue), MAN (red) and seven sites (yellow) located through the trajectory of air from coast do sample sites, described in Fig. 7. The error bars represent the standard deviation of all fluxes and rainfall in Fig. 7 within each trimester, and the numbers represent the number of profiles for the same period for fluxes.

ACPD
9, 17429–17463, 2009

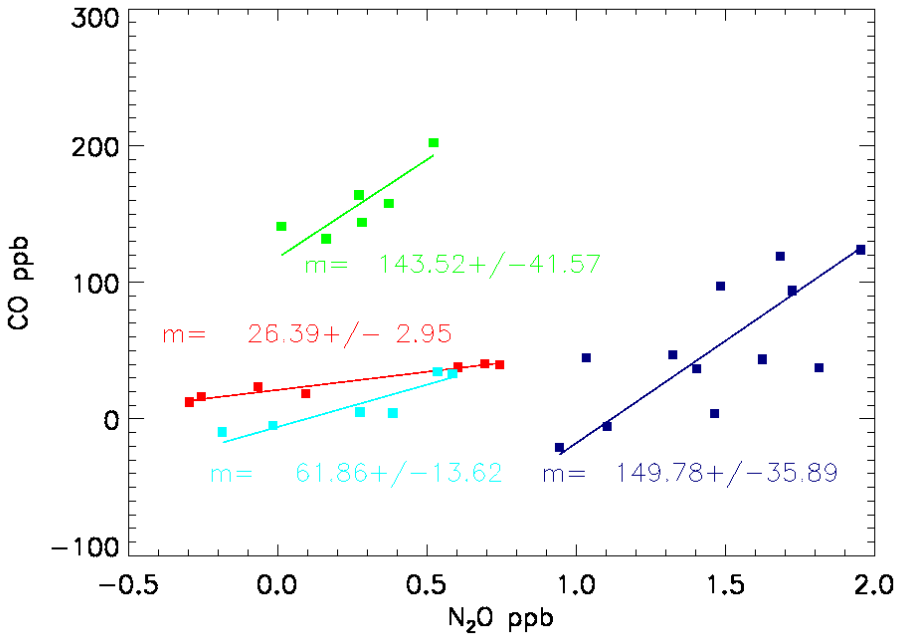

Fig. 10. The 6 higher descendant CO/N_2O ratios obtained for the profiles. The y equation represents the line equation for the points and R^2, the dependence between the variables (CO and N_2O).

ACPD
9, 17429–17463, 2009

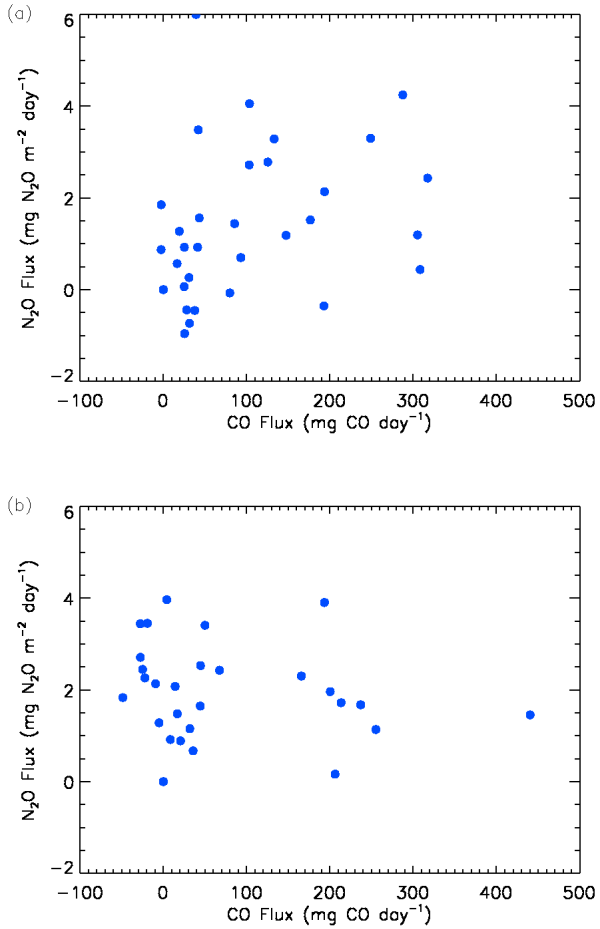

Fig. 11. Correlation between N_2O and CO fluxes during all dry seasons sampled for **(a)** SAN and **(b)** MAN. It is possible observe correlation just at up wind SAN fluxes.

ACPD
9, 17429–17463, 2009